INSTITUTE FOR FUSION STUDIES

DOE/ET-53088-628 IFSR #628

On the Interpretation of Diamagnetic Loop Measurements for a Current-Carrying Plasma Column in a Conducting Chamber

A.N. ALEYNIKOV,[a] B.N. BREIZMAN, V.S. CHERKASSKY,[a] and B.A. KNYAZEV[a]
Institute for Fusion Studies
The University of Texas at Austin
Austin, Texas 78712

FEB 28 1994
OSTI

October 1993

[a] *Budker Institute of Nuclear Physics, 630090 Novosibirsk, Russia*

THE UNIVERSITY OF TEXAS

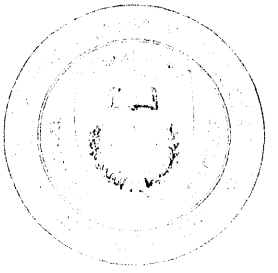

AUSTIN

MASTER

DISTRIBUTION OF THIS DOCUMENT IS UNLIMITED

On the Interpretation of Diamagnetic Loop Measurements for a Current-Carrying Plasma Column in a Conducting Chamber

A.N. Aleynikov,[a] B.N. Breizman, V.S. Cherkassky,[a]
and B.A. Knyazev[a]
Institute for Fusion Studies
The University of Texas at Austin
Austin, Texas 78712

Abstract

A general expression is derived for the signal of a magnetic loop encircling a plasma column inside a conducting chamber with nonuniform current distribution over the plasma cross-section. The ratio of the paramagnetic component to the diamagnetic component of the signal is shown to be independent of the loop radius. Both components increase as the loop radius decreases from the chamber radius to the plasma radius. From the derived expressions, the paramagnetic component of the signal is calculated numerically for several current distributions including those of interest for the experiments. At a given total current, the paramagnetic component of the signal may vary considerably, which generally has to be taken into account in interpreting experimental data. The results of the calculations are used to process the data obtained in the experiments on the SPIN plasma device.

[a]Budker Institute of Nuclear Physics, 630090 Novosibirsk, Russia

I Introduction

Diamagnetic loops, which are often referred to as "magnetic loops," have long become a routine diagnostic tool for measuring the energy content of a magnetically confined plasma.[1, 2, 3] The loop usually encircles the plasma column in order to monitor the time variations of the total magnetic flux, which are caused by the changing plasma pressure. The measurements can be made in a chamber with either perfectly conducting[1] or resistive walls.[4, 5] This technique is also used to measure the parameters of powerful electron beams in experiments on beam propagation and beam plasma heating.[6, 7, 8, 9]

When there is a current in a plasma in addition to the diamagnetic current, the plasma diamagnetism can be obtained by subtracting the current-related paramagnetic part of the loop signal from the total signal. Some additional corrections to the signal, other than the paramagnetic component, have been discussed in Ref. 10. The paramagnetic component is easy to find when the current profile is axisymmetric. However, in the case of an arbitrary profile, the procedure is less straightforward and significant errors may be introduced. Situations with irregular current distributions were clearly observed experimentally at the initial stages of a linear discharge in helium.[10] In these experiments, it was rather difficult to accurately find the plasma temperature in the discharge by the use of data from the magnetic loop and laser interferometer. The need to reduce the uncertainty in the interpretation of the experimental data was the particular motivation for this work.

II Outline of the Experiment and Formulation of the Problem

The scheme of the experiment that we will have in mind in our calculations is shown in Fig. 1. The plasma column of radius R_p is confined in a long cylindrical metal chamber

placed in a longitudinal magnetic field B_0. The length of the chamber L is much larger than its radius R_c. The magnetic loop, a single turn of radius R, is placed inside the chamber at a sufficient distance from the ends of the chamber so that the ends have no effect on the loop signal.

The plasma is created by a pulse discharge between the end electrodes of the chamber. The current j_z of the discharge is generally nonuniform over the plasma cross-section. We assume that the plasma never touches the magnetic loop. The characteristic times for changing the plasma pressure and the current distribution are assumed to be much shorter than the magnetic flux diffusion time, yet sufficiently long for establishing radial equilibrium. Thus, all radial motions are quasistationary, with the sum of the plasma pressure and the magnetic pressure being constant over the plasma cross section. In a long column, this radial balance may depend parametrically on the longitudinal coordinate z.

Changes in the plasma parameters and the current distribution cause variations in the magnetic flux through the cross-section of the loop, which, in turn, induce a loop voltage signal that is measured in the experiment. In what follows we address the question of how sensitive the signal is to the asymmetries in the profile of the plasma current.

III Basic Equations

We start from the equations for plasma equilibrium in a magnetic field:

$$-\nabla p + \frac{1}{c}[\mathbf{j} \times B] = 0 \ , \tag{1}$$

$$\mathrm{rot}\,\mathbf{B} = \frac{4\pi}{c}\mathbf{j} \ , \tag{2}$$

$$\mathrm{div}\,\mathbf{B} = 0 \ . \tag{3}$$

We write the magnetic field as the sum of a strong uniform field B_0 directed along the z-axis of the cylindrical coordinate system and a perturbed field (B_r, B_φ, B_z) that is much smaller

than B_0. We use the transverse components of Eq. (1) to express j_φ and j_r in terms of j_z and to eliminate j_φ and j_r from Eq. (2). Then Eqs. (2) and (3) take the form:

$$-\frac{\partial}{\partial r} B_z + \frac{\partial}{\partial z} B_r = \frac{4\pi}{c} j_z \frac{B_\varphi}{B_0} + \frac{4\pi}{B_0} \frac{\partial p}{\partial r} , \tag{4}$$

$$\frac{1}{r} \frac{\partial}{\partial \varphi} B_z - \frac{\partial}{\partial z} B_\varphi = \frac{4\pi}{c} j_z \frac{B_r}{B_0} - \frac{4\pi}{B_0} \frac{1}{r} \frac{\partial p}{\partial \varphi} , \tag{5}$$

$$\frac{1}{r} \frac{\partial}{\partial r} r B_\varphi - \frac{1}{r} \frac{\partial}{\partial \varphi} B_r = \frac{4\pi}{c} j_z , \tag{6}$$

$$\frac{\partial}{\partial z} B_z + \frac{1}{r} \frac{\partial}{\partial r} r B_r + \frac{1}{r} \frac{\partial}{\partial \varphi} B_\varphi = 0 . \tag{7}$$

We now take into account the very slow change in z-direction of all quantities, which allows us to neglect the term $\partial B_z/\partial z$ in Eq. (7). This can be justified by the following estimates. We assume that both B_φ and B_r are generally of the same order of magnitude as the total transverse magnetic field $B_\perp$. Then Eq. (6) gives

$$j_z \sim B_\perp c/4\pi R_p , \tag{8}$$

where R_p is the plasma radius. By substituting j_z into Eq. (1), we obtain

$$B_z \sim \frac{4\pi p}{B_0} + \frac{B_\perp^2}{B_0} + \frac{B_\perp R_p}{L} , \tag{9}$$

where L is the length of the plasma column. With this estimate for B_z, we find the conditions under which the first term in Eq. (7) is small compared to the other two terms:

$$\frac{R_p}{L} \ll 1 , \tag{10}$$

$$\frac{B_\perp}{B_0} \ll \frac{L}{R_p} , \tag{11}$$

and

$$p \ll \frac{B_0^2}{4\pi} \frac{B_\perp}{B_0} \frac{L}{R_p} \tag{12}$$

Inequalities (10) and (11) are automatically satisfied in a long plasma column. Condition (12), which can be rewritten in terms of the longitudinal current as

$$p \ll \frac{B_0}{c} j_z L \ , \tag{13}$$

is also satisfied in the experiments that we are interested in.

IV Magnetic Flux Through the Loop

In order to calculate the flux

$$\Phi \equiv \int_0^{2\pi} d\varphi \int_0^R B_z \, r dr \ , \tag{14}$$

we multiply Eq. (4) by $\frac{r^2}{2}$ and integrate over the cross-section of the loop, which gives

$$\begin{aligned} &\Phi - \frac{R^2}{2} \int_0^{2\pi} B_z(R) d\varphi + \frac{\partial}{\partial z} \int_0^R \frac{r^2}{2} dr \int_0^{2\pi} B_r \, d\varphi \\ &= -\frac{4\pi}{B_0} \int_0^{2\pi} d\varphi \int_0^R pr \, dr + \frac{2\pi}{cB_0} \int_0^{2\pi} d\varphi \int_0^R r^2 \, j_z \, B_\varphi \, dr \ . \end{aligned} \tag{15}$$

The last term on the left-hand side of this equation equals zero. This can be proved by integrating Eq. (7) with $\partial B_z / \partial z = 0$ over φ, which gives

$$\frac{\partial}{\partial r} \left(r \int_0^{2\pi} B_r \, d\varphi \right) = 0 \ . \tag{16}$$

Since B_r is regular at $r = 0$, we conclude that

$$\int_0^{2\pi} B_r \, d\varphi = 0 \ . \tag{17}$$

The second term on the right-hand side of Eq. (15) can be rewritten as an integral over the loop circumference. In order to make this transformation we use Eq. (6) to express j_z in terms of B_r and B_φ, and then use Eq. (7) with $\partial B_z / \partial z = 0$ to perform integration by parts. The result is

$$\frac{2\pi}{B_0} \int_0^{2\pi} d\varphi \int_0^R r^2 \, j_z \, B_\varphi \, dr = \frac{R^2}{4} \int_0^{2\pi} d\varphi \left(B_\varphi^2 - B_r^2 \right) \Big|_{r=R} \ . \tag{18}$$

We now express the second term on the left-hand side of Eq. (15) in terms of Φ by using the condition that the total magnetic flux inside the conducting chamber is conserved and also the fact that $\int_0^{2\pi} B_z\, d\varphi$ does not depend on r in the vacuum region between the loop and the conducting wall:

$$\int_0^{2\pi} B_z(R) d\varphi = \frac{2}{R_c^2 - R^2} (\Phi_0 - \Phi) \ . \tag{19}$$

Here, Φ_0 is the given flux inside the chamber. Finally, we combine Eqs. (15) and (17)–(19) to obtain the following expression for the perturbed magnetic flux through the loop:

$$\Phi = -\frac{R_c^2 - R^2}{R_c^2} \frac{4\pi}{B_0} \left[\int_0^R p\, dS - \frac{R^2}{16\pi} \int_0^{2\pi} d\varphi (B_\varphi^2 - B_r^2)\Big|_{r=R} \right] + \frac{R^2}{R_c^2} \Phi_0 \ . \tag{20}$$

The first integral in Eq. (20) characterizes the plasma diamagnetism, while the second one corresponds to the paramagnetic effect from the longitudinal current. The last term in Eq. (20) is an insignificant constant that can be dropped since it does not contribute to the time derivative of the flux.

For an axisymmetric longitudinal current, the B_r^2 term in Eq. (20) equals zero. In this case, the integral of B_φ^2 only depends on the total plasma current I and is given by

$$\int_0^{2\pi} B_\varphi^2\, d\varphi \equiv P_0 = 8\pi I^2 / c^2 R^2 \ . \tag{21}$$

This is the paramagnetic contribution that is typically used in processing experimental data. Modification of this term due to asymmetry of the current can be described by the coefficient

$$q \equiv q_\varphi + q_r \equiv \frac{\int d\varphi B_\varphi^2(R,\varphi)}{P_0} - \frac{\int d\varphi B_r^2(R,\varphi)}{P_0} \ . \tag{22}$$

For an axisymmetric current, we have $q_\varphi = 1$ and $q_r = 0$.

V Paramagnetic Effect from the Longitudinal Current

In order to calculate the paramagnetic contribution, we solve Eqs. (6) and (7) for B_φ and B_r with a given current j_z and with $\frac{\partial}{\partial z} B_z = 0$. We introduce the vector potential A so that

$$B_r = -\frac{1}{r}\frac{\partial A}{\partial \varphi}\,, \qquad B_\varphi = \frac{\partial A}{\partial r}\,. \tag{23}$$

Then Eq. (6) reduces to

$$\frac{1}{r}\frac{\partial}{\partial r} r \frac{\partial A}{\partial r} + \frac{1}{r^2}\frac{\partial^2 A}{\partial \varphi^2} = \frac{4\pi}{c} j_z\,. \tag{24}$$

We expand j_z and A into Fourier series,

$$\begin{aligned} j_z &= j_0(r) + \sum_{\ell=1}^{\infty} \left(j_\ell^+(r)\cos\ell\varphi + j_\ell^-(r)\sin\ell\varphi \right) \\ A &= A_0(r) + \sum_{\ell=1}^{\infty} \left(A_\ell^+(r)\cos\ell\varphi + A_\ell^-(r)\sin\ell\varphi \right)\,, \end{aligned} \tag{25}$$

to obtain the following equations for the Fourier components:

$$\begin{aligned} &\frac{1}{r}\frac{\partial}{\partial r} r \frac{\partial A_0}{\partial r} = \frac{4\pi}{c} j_0\,, \\ &\frac{1}{r}\frac{\partial}{\partial r} r \frac{\partial}{\partial r} A_\ell^+ - \frac{\ell^2}{r^2} A_\ell^\pm = \frac{4\pi}{c} j_\ell^\pm\,. \end{aligned} \tag{26}$$

The functions $A_\ell^\pm$ must satisfy the boundary condition

$$A_\ell^\pm(R_c) = 0\,, \tag{27}$$

which corresponds to having $B_r = 0$ at the wall of the conducting chamber. Also, A_0 and $A_\ell^\pm$ must be regular at $r = 0$. The corresponding solution of Eq. (26) has the form

$$\frac{\partial A_0}{\partial r} = \frac{4\pi}{cr}\int_0^r r\, j_0(r)dr\ ,$$

$$A_\ell^{\pm}(r) = \frac{2\pi}{c\ell}\left[- r^\ell \int_r^{R_c} \frac{j_\ell^{\pm}\, r dr}{r^\ell} + \frac{1}{R_c^\ell}\left(\frac{r}{R_c}\right)^\ell \int_0^{R_c} j_\ell^{\pm}\, r^{\ell+1} dr \right.$$

$$\left. - \frac{1}{r^\ell}\int_0^r j_\ell^{\pm}\, r^{\ell+1} dr \right] . \tag{28}$$

We now note that the paramagnetic factor q is determined by the magnetic field components at the loop radius, that is, in the vacuum region between the plasma boundary and the conducting wall. In this region $j_\ell^{\pm}(r) = 0$, which simplifies Eq. (28) to

$$\begin{aligned} \frac{\partial A_0}{\partial r} &= \frac{4\pi}{cr}\int_0^r r\, j_0(r)dr \\ A_\ell^{\pm} &= \frac{2\pi}{c\ell}\frac{1}{R_c^\ell}\left(\int_0^{R_c} j_\ell^{\pm}\, r^{\ell+1} dr\right)\left[\left(\frac{r}{R_c}\right)^\ell - \left(\frac{R_c}{r}\right)^\ell\right] . \end{aligned} \tag{29}$$

Finally, we combine Eqs. (22), (23), (25), and (29) to obtain

$$q = 1 + \frac{1}{2}\sum_{\ell=1}^{\infty}\left[\left(\frac{\int_0^{R_c} j_\ell^{+}\, r^{\ell+1} dr}{R_c^\ell \int_0^{R_c} j_0 r\, dr}\right)^2 + \left(\frac{\int_0^{R_c} j_\ell^{-}\, r^{\ell+1} dr}{R_c^\ell \int_0^{R_c} j_0 r\, dr}\right)^2\right] . \tag{30}$$

It should be noted that the q-factor is a function of r/R_c only and does not depend on the loop radius R. This factor is positive definite, which shows that the longitudinal current produces only a paramagnetic and never a diamagnetic effect. Moreover, q is always larger than unity; it only equals unity for an axisymmetric current. Hence, processing experimental data under the assumption that the current is axisymmetric is actually a way to obtain a limitation from below on the plasma pressure.

VI Calculation of the q-Factor for Experimental Data Processing

In order to get a preliminary idea of the role of current asymmetry, we calculate q analytically for an off-axis delta-function current,

$$j_z(r,\varphi) = \frac{I}{\rho}\,\delta(\varphi)\delta(r-\rho)\ ,$$

where ρ is the radial position of the current. In this case

$$j_0^+ = \frac{I}{\pi\rho}\,\delta(r-\rho)\ , \tag{31}$$

$$j_0 = \frac{I}{2\pi\rho}\,\delta(r-\rho)\ , \tag{32}$$

$$j_\ell^- = 0\ , \tag{33}$$

and Eq. (30) reduces to

$$q = \frac{2}{1-\left(\frac{\rho}{R_c}\right)^2} - 1 = \frac{2}{1-\left(\frac{\rho}{R}\right)^2\left(\frac{R}{R_c}\right)^2} - 1\ ,\ \rho < R\ . \tag{34}$$

This q-factor is shown by the dotted line in Fig. 2. It follows from Eq. (34) that, when the current comes close to the loop, q grows to its maximum value

$$q_{\rho=R} = \frac{1+\left(\frac{R}{R_c}\right)^2}{1-\left(\frac{R}{R_c}\right)^2}\ . \tag{35}$$

For example, for the case[10, 11] of $R/R_c = 0.86$ we get $q_{\rho=R} = 6.8$.

Also shown in Fig. 2 is the q-factor for another typical current configuration — a circular segment of an apex angle $\Delta\varphi$ with different values of $\Delta\varphi$. It is easy to see that the greater the current asymmetry, the stronger the paramagnetic effect. To analyze the role of the paramagnetic component in the measurements of plasma diamagnetism, we rewrite Eq. (20)

in the following form:

$$\Delta\Phi = -\frac{R_c^2 - R^2}{R_c^2}\,\frac{4\pi\int_0^R p\,dS}{B_0}\left[1 - \frac{I^2 q}{2c^2\int_0^R p\,dS}\right]. \tag{36}$$

It follows from Eq. (36) that the farther the loop is from the wall, the larger the useful signal is. Since the q-factor is constant for a given current distribution, the ratio of the paramagnetic to the diamagnetic component of the signal does not depend on the loop radius. For these reasons, the loop should be placed as close to the plasma as possible. However, under real experimental conditions, one should take into account that electrostatic induction may grow if the loop is close to the plasma.

The calculation of q for a given current profile generally requires a numerical procedure. These calculations can be performed either by the use of Eq. (30) or by a direct integration of the experimentally obtained current distribution over the plasma cross-section. For the calculation of q, we have developed a code that is written in Turbo Pascal for an IBM PC. The procedure used in the code is described in the Appendix. To test the code, we calculate q for an off-axis delta-function current distribution and circular segments. The results have been found to agree with those shown in Fig. 2.

The code has been used to evaluate q for the experimentally obtained current profiles of a linear discharge in helium. The experimental setup and diagnostics are described in Refs. 10, 11, and 12. The plasma was produced in a 10.4-cm diameter stainless-steel tube in a 4.4 T longitudinal magnetic field by the discharge between the end electrodes. The discharge cross-section was limited by a glass diaphragm, 8 cm in diameter. The plasma pressure was inferred from the signals of two magnetic loops, each 9 cm in diameter.

Figure 3 shows the RC-integrated signal of a magnetic loop $W_\perp$, which contains both diamagnetic and paramagnetic components. The paramagnetic component was calculated, assuming axial symmetry, from the total current trace I_{tot}. We then found the plasma paramagnetism $\int n_e T dS$ by subtracting this value from $W_\perp$. With plasma density n_e measured

by means of laser interferometer, one can find the behavior of the plasma temperature T_e (see Ref. 10 for details).

The procedure outlined above is commonly used for the calculation of the plasma diamagnetism, but it fails in the case of a nonaxisymmetric current. The magnitude of the diamagnetism obtained in this way is only correct when the current is either almost symmetric or negligibly small (triangles in Fig. 3). In general, in order to obtain the correct value of the diamagnetism, one should consider the actual distribution of the plasma current. In Ref. 10 an asymmetry has been observed in the pictures of plasma self-luminosity taken with a long-focus optical system[12] with a time-resolved electron-optic image converter.

Plasma cross-sections at times $3\mu s$ and $17\mu s$ are shown in Fig. 4. The figure demonstrates that the plasma becomes axisymmetric when the discharge is well developed. However, there is no axial symmetry in the initial stage of the discharge, and the plasma shape varies from pulse to pulse. For the plasma shape shown in Fig. 4 (left) and for the dimensions of plasma and chamber listed previously, the nonaxisymmetric correction to the paramagnetism increases the value of the diamagnetism by 22%. The corrected values of the diamagnetism at $3\mu s$ and $17\mu s$ are shown in Fig. 3 by circles. The error bars represent the dispersion of the diamagnetism at $3\mu s$ due to pulse-to-pulse variations of the plasma shape.

VII Acknowledgments

The authors are grateful to D.D. Ryutov for helpful discussions, to P.I. Melnikov for his assistance in collecting and processing the experimental data, and to J.W. Van Dam for editing the manuscript.

Appendix

With the current distribution known from the experiments and recorded into a two-dimensional array, we use the following procedure to calculate the q-factor defined by Eq. (22). Since q is independent of the loop radius R we can rewrite Eq. (22) in the form

$$q = \frac{\int d\varphi B_\varphi^2(R,\varphi)}{P_0} - \frac{\int d\varphi B_r^2(R,\varphi)}{P_0} = \frac{\int d\varphi B_\varphi^2(R_c,\varphi)}{P_0} \,. \tag{A1}$$

We now find B_φ by using Eq. (23), with the vector potential A obtained by the method of images,[13]

$$A(r,\varphi) = \int dA(r,\varphi;r_i,\varphi_i) = -\frac{1}{c}\int j(r_i,\varphi_i) r_i dr_i d\varphi_i \ln r^2$$

$$+ r_i^2 - 2rr_i \cos \frac{(\varphi-\varphi_i)}{r^2 + R_c^4/r_i^2 - 2r(R_c^2/r_i)\cos(\varphi\varphi_i)} \tag{A2}$$

with the boundary condition $A(R_c,\varphi) = \text{const}$, where r_i and φ_i are referred to the current elements.

By introducing dimensionless variables

$$\tilde{R} = R_c/R,\ \tilde{r} = r_i/R,\ \tilde{\varphi} = \varphi - \varphi_i,\ \tilde{j}(\tilde{r},\varphi_i) = \frac{R^2 j(\tilde{r},\varphi_i)}{I} \,,$$

with

$$\int j(\tilde{r},\varphi_i)\, \tilde{r} d\tilde{r} d\varphi_i = 1 \,,$$

we finally obtain

$$B_\varphi(R_c,\varphi) = \int_0^1 \int_{-\pi}^{\pi} \frac{I}{cR_c} \tilde{j}(\tilde{r},\varphi_i) \tilde{r}\, d\tilde{r} d\varphi_i \frac{2(1-\tilde{r}^2)}{1 - 2\tilde{r}\cos\tilde{\varphi} + \tilde{r}^2} \,. \tag{A3}$$

References

[1]L.V. Brzhechko, O.S. Pavlichenko, and O.M. Shvets, Soviet Atomic Energy **20**, 62 (1966), and Plasma Phys. (J. Nucl. Energy Part C) **8**, 799 (1966).

[2]M.A. Rothman, Plasma Phys. **10**, 86 (1968).

[3]V.S. Mukhovatov and V.D. Shafranov, Nucl. Fusion **11**, 605 (1971).

[4]U.V. Gott and R.I. Sobolev, in *Plasma Diagnostics* (Atomizdat, Moscow, 1973), Vol. 3, p. 525 (in Russian).

[5]J.H. Booske, W.D. Getty, and R.M. Gilgenbach, Plasma Phys. and Controlled Fusion **28**, 1449 (1986).

[6]Yu.I. Abrashitov, V.S. Koydan, V.V. Konyukhov, V.M. Lagunov, V.N. Lukyanov, K.I. Mekler, and D.D. Ryutov, Sov. Phys. JETP **39**, 647 (1974).

[7]A.A. Kim, Ph. D. Thesis, Tomsk, 1983.

[8]M.L. Sloan and H.A. Davis, Phys. Fluids **25**, 2337 (1982).

[9]V.I. Erofeev, B.A. Knyazev, S.V. Lebedev, and V.V. Chikunov, Sov. Phys. Tech. Phys. **34**, 1156 (1989).

[10]B.A. Knyazev, P.I. Melnikov, and V.V. Chikunov, "Characteristics of Plasma Produced by a Linear Discharge in the Metal Chamber of the SPIN Device," to be published in Sov. Phys. Tech. Phys. (1993).

[11]B.A. Knyazev, P.I. Melnikov, and V.V. Chikunov, Sov. J. Plasma Phys. **16**, 836 (1990).

[12]B.A. Knyazev, P.I. Melnikov, and V.V. Chikunov, Sov. Phys. Tech. Phys. **60**, 1140 (1990).

[13]L.D. Landau and E.M. Lifshitz, *Electrodynamics of Continuous Media*, 2nd ed., (Oxford, Univ. Press, Oxford, 1984).

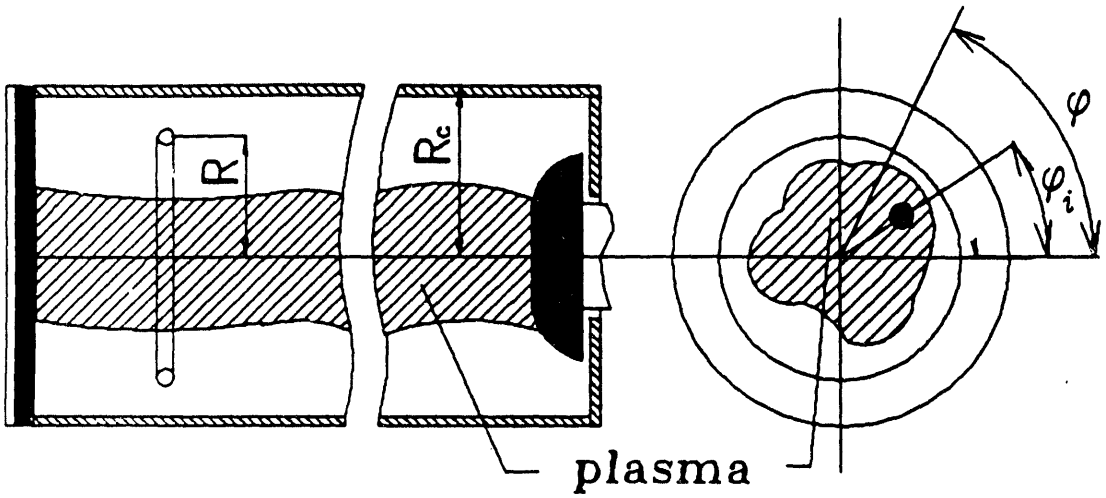

Fig. 1. Experimental configuration for measuring plasma diamagnetism.

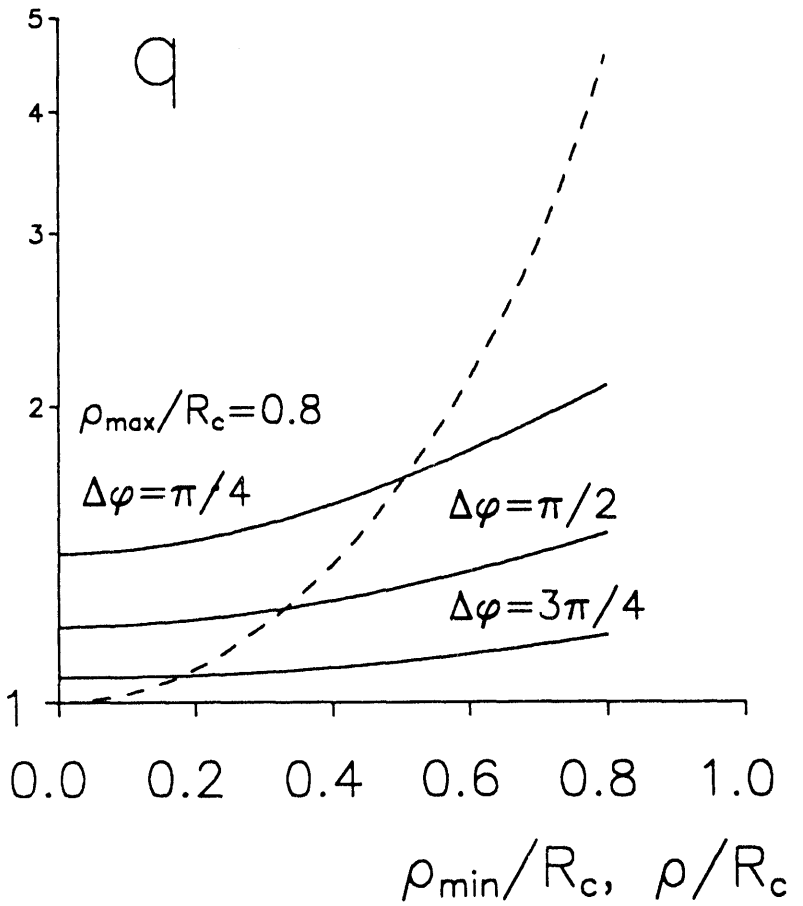

Fig. 2. Dependence of the q-factor on the distribution of longitudinal plasma current. Dotted line shows the q-factor for a localized current as a function of its position ρ/R_c; solid lines show the q-factor for a current that is uniform within a circular segment with outer radius $\rho_{max}/R_c = 0.8$ and varying inner radius ρ_{min}/R_c (three lines correspond to three different values of the apex angle $\Delta\varphi$).

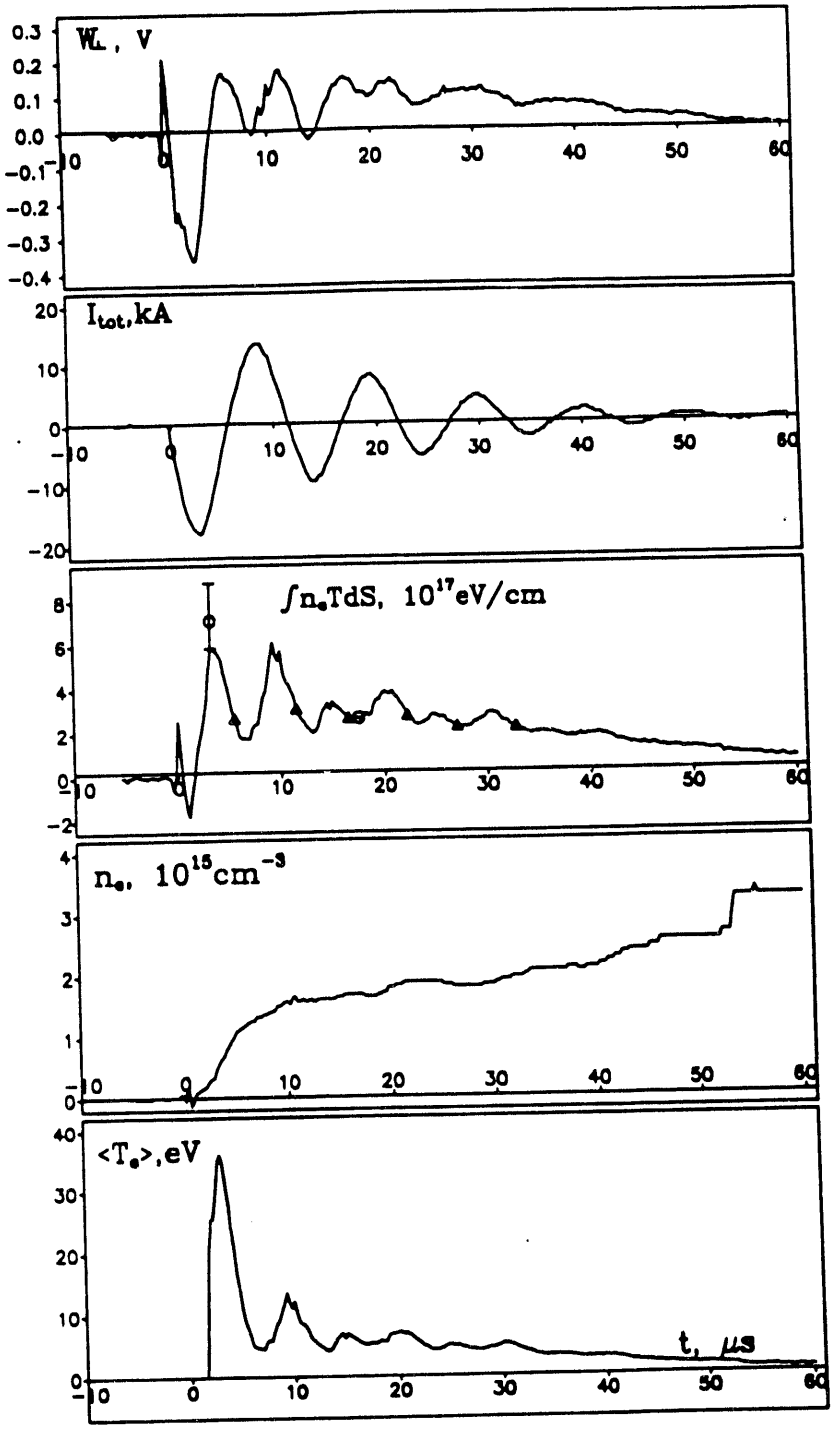

Fig. 3. Integrated magnetic loop signal ($W_\perp$), total plasma current (I_{tot}), and the results of processing the experimental data: plasma diamagnetism ($\int n_e T dS$), density (n_e), and temperature (T_e).

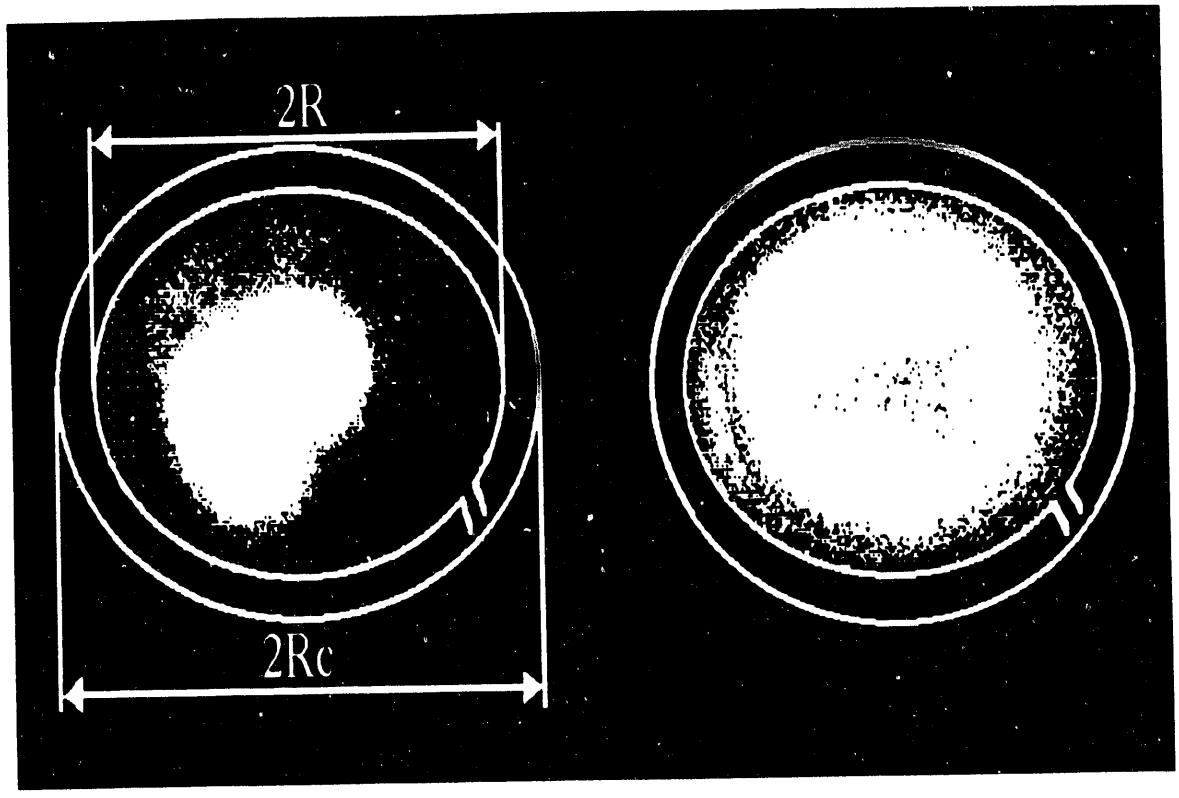

Fig. 4. Plasma self-luminosity at two stages of the linear discharge (cross-section view): left-initial stage of the discharge (3 μs); right-well developed discharge (17 μs).

END

DATE
FILMED
3/18/94